Spontaneous neural activity during human slow wave sleep

Thien Thanh Dang-Vu[†‡§], Manuel Schabus[†], Martin Desseilles[†], Geneviève Albouy[†], Mélanie Boly[†‡], Annabelle Darsaud[†], Steffen Gais[†], Géraldine Rauchs[†], Virginie Sterpenich[†], Gilles Vandewalle[†], Julie Carrier[¶], Gustave Moonen[‡], Evelyne Balteau[†], Christian Degueldre[†], André Luxen[†], Christophe Phillips[†], and Pierre Maquet[†‡]

[†]Cyclotron Research Centre, University of Liège, B4000 Liège, Belgium; [‡]Department of Neurology, CHU Sart Tilman, B4000 Liège, Belgium; and [¶]Department of Psychology, University of Montreal, Montreal, QC, Canada H2V 2S9

Edited by Marcus E. Raichle, Washington University School of Medicine, St. Louis, MO, and approved July 11, 2008 (received for review February 26, 2008)

Slow wave sleep (SWS) is associated with spontaneous brain oscillations that are thought to participate in sleep homeostasis and to support the processing of information related to the experiences of the previous awake period. At the cellular level, during SWS, a slow oscillation (<1 Hz) synchronizes firing patterns in large neuronal populations and is reflected on electroencephalography (EEG) recordings as large-amplitude, low-frequency waves. By using simultaneous EEG and event-related functional magnetic resonance imaging (fMRI), we characterized the transient changes in brain activity consistently associated with slow waves (>140 μV) and delta waves (75–140 μV) during SWS in 14 non-sleep-deprived normal human volunteers. Significant increases in activity were associated with these waves in several cortical areas, including the inferior frontal, medial prefrontal, precuneus, and posterior cingulate areas. Compared with baseline activity, slow waves are associated with significant activity in the parahippocampal gyrus, cerebellum, and brainstem, whereas delta waves are related to frontal responses. No decrease in activity was observed. This study demonstrates that SWS is not a state of brain quiescence, but rather is an active state during which brain activity is consistently synchronized to the slow oscillation in specific cerebral regions. The partial overlap between the response pattern related to SWS waves and the waking default mode network is consistent with the fascinating hypothesis that brain responses synchronized by the slow oscillation restore microwake-like activity patterns that facilitate neuronal interactions.

fMRI | neuroimaging | sleep physiology | slow oscillation

During the deepest stage of nonrapid eye movement (NREM) sleep, also referred to as slow wave sleep (SWS) in humans (stage 3–4 of sleep), spontaneous brain activity is organized by specific physiological rhythms, the neural correlates of which have been described in animals (1). Unit recordings have shown that neuronal activity during SWS is characterized by a fundamental oscillation of membrane potential. This so-called "slow oscillation" (<1 Hz) is recorded in all major types of neocortical neurons during SWS and is composed of a depolarizing phase, associated with important neuronal firing ("up state"), followed by a hyperpolarizing phase during which cortical neurons remain silent for a few hundred milliseconds ("down state") (2, 3). The slow oscillation occurs synchronously in large neuronal populations in such a way that it can be reflected on electroencephalography (EEG) recordings as large-amplitude, low-frequency waves (4).

Delta rhythm (1–4 Hz) is another characteristic oscillation of NREM sleep. The neural underpinnings of delta rhythm remain uncertain, however. In the dorsal thalamus, a clock-like delta rhythm is generated by the interplay of two intrinsic membrane currents, although another delta rhythm survives complete thalamectomy, suggesting a cortical origin (1).

In humans, a slow oscillation was identified on scalp EEG recordings by the recurrence of spindles (5) or their grouping by slow waves (6), or as high-amplitude slow waves (7). Scalp EEG recordings demonstrated the spatial variability of slow waves. Each wave originates at a specific site and travels over the scalp following a particular trajectory (7). Although waves originate more frequently in frontal regions, brain areas consistently recruited by the slow oscillation have not yet been identified.

In addition, the taxonomy of SWS waves is not always clear in humans. The power density in the 0.75–4 Hz frequency band, usually referred to as *slow wave activity* (SWA), has proven to be a very useful and popular parameter, because it quantifies the dissipation of homeostatic sleep pressure during NREM sleep (8). However, its frequency bounds do not respect the dichotomy between slow (<1 Hz) and delta rhythms (1–4 Hz) that is based on differences in the respective cellular correlates of these oscillations in animals (1). In the temporal domain, the amplitude of SWS waves is classically >75 μV (9). However, the largest waves (>140 μV) were recently taken as realizations of the slow oscillation (<1 Hz) (6, 7). This approach tacitly implies that waves of intermediate amplitude (between 75 and 140 μV) correspond to delta waves and implicitly assumes that slow waves and delta waves are two distinct processes. This concept contrasts with the view, promoted by computational models that slow waves and delta waves are both underpinned by the cellular processes underlying the slow oscillation (10).

In this work, our first objective was to identify the brain areas that consistently increase their activity in relation to SWS waves. Identifying those responses to SWS waves would speak for their constant recruitment during these waves. Our second aim was to assess the similarities and differences between slow and delta waves, operationally defined on amplitude criteria. This information would contribute to a better understanding of human NREM sleep oscillations. To address these issues, we used simultaneous EEG/fMRI and an event-related design to characterize the functional brain correlates of slow waves and delta waves during SWS in normal human volunteers. Importantly, participants were not sleep-deprived, which allowed us to study sleep under normal homeostatic pressure. SWS waves were considered identifiable neural events and categorized into high-amplitude slow waves (>140 μV), as described by Massimini *et al.* (7), and slow waves of lower amplitude, which we refer to as delta waves (75–140 μV). In the analysis of fMRI data, both types of waves were taken as events and compared with the SWS baseline activity, to identify the brain areas that would systematically respond to the occurrence of the detected waves.

Results

Of 25 volunteers, 14 were able to generate stable NREM sleep episodes in the scanner. The mean duration of NREM sleep (stages

Author contributions: T.T.D.-V., E.B., C.D., A.L., C.P., and P.M. designed research; T.T.D.-V., M.S., M.D., G.A., M.B., A.D., S.G., G.R., V.S., G.V., J.C., and P.M. performed research; T.T.D.-V. and P.M. analyzed data; and T.T.D.-V., G.M., and P.M. wrote the paper.

This article is a PNAS Direct Submission.

[§]To whom correspondence should be addressed. E-mail: tt.dangvu@ulg.ac.be

The authors declare no conflicts of interest.

This article contains supporting information online at www.pnas.org/cgi/content/full/0801819105/DCSupplemental.

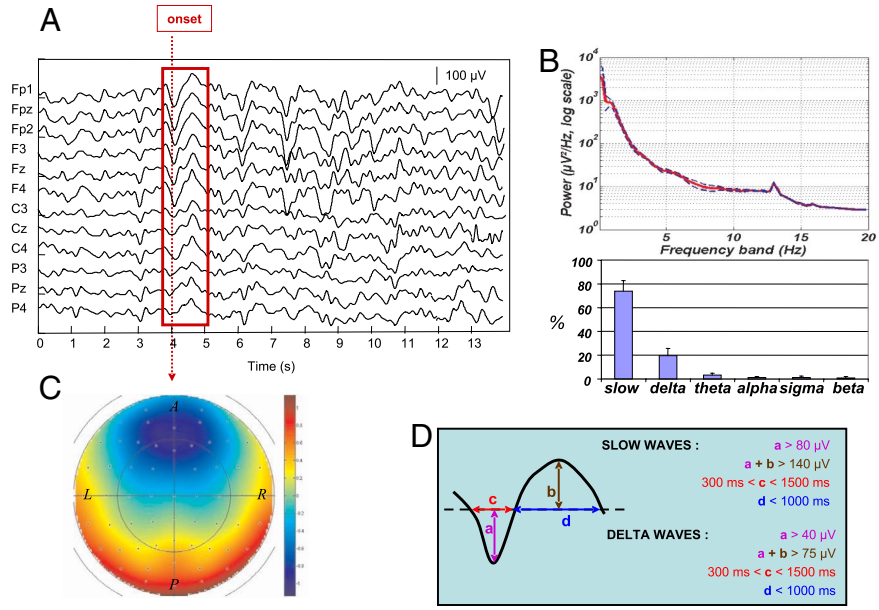

Fig. 1. EEG detection of slow oscillation. (*A*) 14 second epoch of NREM sleep after artifact correction. For display, data from 12 channels were referenced to average mastoids and bandpass-filtered between 0.1 and 20 Hz. A typical slow wave is framed in red to indicate the onset positioned at the peak negativity. (*B*) (*Upper*) Power spectrum (0.1–20 Hz) of SWS epochs averaged over all subjects. Prominent frequency ranges are below 4 Hz. Power spectra were computed on Fz (fast Fourier transform, Hamming window; average of 4-s windows overlapping by 2 s). Power values are displayed by using a logarithmic scale. The blue dotted lines are the standard error curves. (*Lower*) Proportion of EEG power in each frequency band, expressed as the percentage of the EEG power in a specific frequency band over the total EEG power across all SWS epochs and all subjects (means and standard deviations). Frequency bands are slow (<1 Hz), delta (1–4 Hz), theta (4–8 Hz), alpha (8–11 Hz), sigma (11–15 Hz), and beta (15–20 Hz). Slow and delta frequency bands account for 93% of the total EEG power. (*C*) Slow wave scalp topography. Normalized values of potential amplitudes on all 64 EEG channels at times corresponding to the peak negativity of slow waves were averaged over detected slow waves and subjects. Note the clear frontal dominance of the slow waves, which is consistent with other studies (7). For the calculation of this map, we used the average reference. The vertical bar indicates the color code for normalized potential values. A, anterior; P, posterior; L, left; R, right. The delta wave scalp topography map is highly similar to the slow wave map and thus the data is not shown. (*D*) Criteria used for automatic detection of slow waves and delta waves (7).

2–4) was 46.7 min per subject, ranging from 6.1–96.1 min. The mean NREM sleep latency was 19.1 min, ranging from 4.7–28.9 min. For the analysis of each individual data set, epochs of uninterrupted SWS (stage 3–4), devoid of any arousals or movement times, were selected following classical sleep criteria (9). These epochs ranged from 2.46–36.1 (mean, 10.8) min. Spectral power analyses were conducted on these SWS epochs across subjects and, as expected, showed prominent activity within frequency band inferior to 4 Hz, that accounted for 93.2% of the total EEG power (Fig. 1*B*). The residual EEG power was distributed between theta (4–8 Hz; 3.4%), alpha (8–11 Hz; 1.3%), sigma (11–15 Hz; 1.4%), and beta (15–20 Hz; 0.7%) frequency bands.

Slow waves and delta waves were automatically detected on the selected SWS epochs (7) and verified visually (Fig. 1 *A* and *D*). The onset of each wave was positioned at the maximum negativity of the wave (Fig. 1*A*, red dotted arrow), because it is considered to reflect the transition to the depolarizing phase or up state of the intracellularly defined slow oscillation (7). The number of events (i.e., detected waves) per subject ranged from 19–689 (mean, 223) for slow waves and from 18–557 (mean, 193) for delta waves. The average scalp topographical distribution of EEG potentials taken at the onsets of slow waves showed a clear frontal predominance (Fig. 1*C*), consistent with the frontal predominance of SWA (8) and the greater probability of detecting slow waves over frontal channels (7). A similar map was obtained for delta waves (data not shown).

The analysis of fMRI data acquired simultaneously allowed us to assess the brain activities associated with the onset of all detected slow waves and/or delta waves. The resulting functional maps show the neural activities recruited by these events compared with the baseline activity of SWS, taking into account the variance explained by sleep spindles. The baseline activity consisted essentially of small-amplitude oscillations above the low-frequency ranges (>4 Hz), representing no more than 7% of the total sleep EEG power (over Fz; Fig. 1*B*).

We first identified the brain areas in which the detected waves, both slow waves and delta waves, were systematically associated with an increase in local activity (main effect of all waves). We found significant brain activity increases in the pontine tegmentum (in an area encompassing the locus coeruleus), midbrain, cerebellum, parahippocampal gyrus, inferior frontal gyrus, middle frontal gyrus, precuneus, and posterior cingulate cortex (Table 1; Fig. 2). We then assessed the brain responses that were selectively associated with slow waves or delta waves (main effect of either wave, relative to baseline). Slow waves were related to significantly increased brain activity in the pons, cerebellum, and parahippocampal gyrus (Table 2; Fig. 3, *Left*). Delta waves were associated with significantly increased brain activity in the medial prefrontal cortex and inferior frontal gyrus (Table 3; Fig. 3, *Right*). Importantly, in none of these contrasts was the regional brain activity significantly decreased in association with slow waves and/or delta waves. Finally, we directly compared the brain responses related to slow waves and delta waves, but found no significant difference between them.

All of the reported activations were specifically related to the presence of the detected waves, but not to a specific phase of the wave. Indeed, moving the onset of each wave to, for instance, the maximum positivity of the wave led to identical brain activations (data not shown). Our results are indisputably related to the presence of the waves; however, by using random onset positions within the selected NREM sleep epochs produced no significant fMRI results.

Table 1. Brain regions activated in relation to slow oscillation: Common effects of high-amplitude slow waves and delta waves

Brain region	*x*	*y*	*z*	*P*	*Z* score
Brainstem (midbrain) (40, 41)	−12	−22	−8	0.015	3.74
Brainstem (pons) (40, 41)	−12	−40	−28	0.001	4.43
Left cerebellar hemisphere (42)	−42	−62	−34	0.006	4.04
Right cerebellar hemisphere (42)	38	−68	−34	0.012	3.84
Right parahippocampal gyrus (19)	22	−40	−26	0.001	4.54
Left inferior frontal gyrus (13)	−38	26	−18	0.002	4.39
Right inferior frontal gyrus (13)	42	24	−16	0.048	3.41
Left precuneus (43)	−4	−50	50	0.033	3.54
Right posterior cingulate cortex (40)	8	−60	20	0.04	3.47

Here the *x*, *y*, and *z* values are coordinates in the MNI space. The *z* scores result from the statistical parametric analysis; *p* refers to the probability of the null hypothesis (i.e., absence of activity change associated with slow oscillation; $P < .05$), after correction for multiple comparisons on a volume of interest centered on published coordinates [reference(s) specified for each brain area]. Additional results that did not survive correction for multiple comparisons are given in Table S1.

NEUROSCIENCE

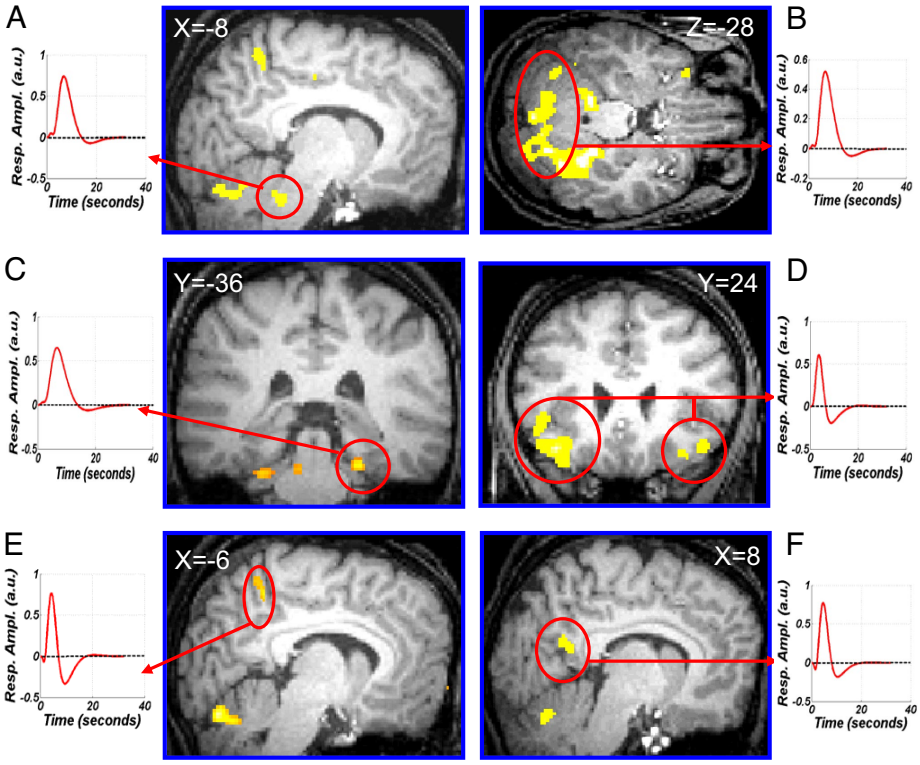

Fig. 2. fMRI results. Brain regions activated in relation to slow oscillation: common effects of both high-amplitude slow waves and delta waves. (*Middle*) Significant responses associated with both slow waves and delta waves. Functional results are displayed on an individual structural image (display at $P < .001$, uncorrected), at different levels of the *x*, *y*, and *z* axes, as indicated for each section. (*Left* and *Right*) Time course (in seconds) of fitted response amplitudes (in arbitrary units) during slow waves or delta waves in the corresponding circled brain area. All responses consist of regional increases in brain activity. (*A*) Pontine tegmentum. (*B*) Cerebellum. (*C*) Right parahippocampal gyrus. (*D*) Inferior frontal gyrus. (*E*) Precuneus. (*F*) Posterior cingulate cortex.

Discussion

In this study, brain response patterns associated with characteristic neural events of SWS (i.e., slow waves and delta waves) were characterized in non-sleep-deprived volunteers by using EEG/fMRI. Our results can be summarized in three main findings. First, the event-related design allowed us to detect significant *increases* in regional brain activity associated with slow waves and delta waves in both subcortical and cortical areas, whereas no decreases in activity were observed. Second, a direct comparison of slow waves and delta waves revealed no significant difference between the activities associated with these waves; however, when compared with baseline activity, slow waves were selectively associated with responses in the brainstem, cerebellum, and parahippocampal gyrus, and delta waves were related to frontal responses. Third, a partial overlap was found between the default network reported during resting wakefulness (11) and responses associated with SWS oscillations.

Comparison with Earlier Positron Emission Tomography and fMRI Studies. Our results confirm our hypothesis that deep NREM sleep is characterized at the macroscopic systems level by phasic increases in regional brain activity in relation to discrete events as slow waves or delta waves. These results stand in sharp contrast with earlier studies of NREM sleep by using positron emission tomography (PET) (12) or block-design fMRI (13), which found decreased brain activity during NREM sleep. This discrepancy can be attributed to two main factors. The statistical contrasts used in many of these earlier studies compared the distribution of brain activity during sleep and wakefulness. In contrast, our analysis describes the transient changes in regional brain activity associated with discrete SWS waves relative to a baseline consisting of low-power theta, alpha, and beta activity during NREM sleep. We emphasize that the increased brain activities related to the waves detected in the present study were contrasted with the baseline activity of SWS and do not imply a comparison with waking activity. Second, because of its low temporal resolution, PET is poorly adapted to detect transient brain activities compared with event-related fMRI. For example, the negative correlation between thalamic blood flow and power within the spindle frequency range observed with PET (14) likely was due to averaging of various neural events, including up and down states, over the entire scanning time. In the present study, the temporal resolution of fMRI allowed the detection of activation related to the occurrence of slow waves or delta waves but was not precise enough to identify the brain responses specifically related to the phase of the waves, that is, the respective effects of the up and down states. Other fMRI studies have shown decreased brain activity associated with NREM sleep waves (delta power and K complexes) (15), but these were stimulus-induced waves, not spontaneous waves as reported here.

Table 2. Brain regions specifically activated in relation to high-amplitude slow waves

Brain region	*x*	*y*	*z*	*P*	*Z* score
Brainstem (pons) (41)	−14	−40	−28	0.025	3.63
Left cerebellar hemisphere (13)	−48	−66	−32	0.006	4.03
Right cerebellar hemisphere (13)	36	−62	−26	0.047	3.42
Right parahippocampal gyrus (19)	24	−36	−26	0.003	4.21
Left parahippocampal gyrus (19)	−24	−34	−28	0.014	3.81

Here the *x*, *y*, and *z* values are coordinates in the MNI. The *Z* scores result from the statistical parametric analysis; *P* refers to the probability of the null hypothesis (i.e., absence of activity change associated with high-amplitude slow waves; $P < .05$), after correction for multiple comparisons on a volume of interest centered on published coordinates (reference specified for each brain area). Additional results that did not survive correction for multiple comparisons are given in Table S2.

Functional Segregation of Brain Responses Associated with SWS Oscillations. Our findings provide a characterization of the neural correlates of SWS oscillations that complements the description obtained from scalp EEG in humans or cellular recordings in animals. Unit recordings in the naturally sleeping cat or in brain slices have indicated that the slow oscillation is generated within the cortex (4, 16) and can be recorded from all cortical areas (1). In contrast, the cortical activities associated with SWS oscillations, although widespread, are not global; rather, they have been iden-

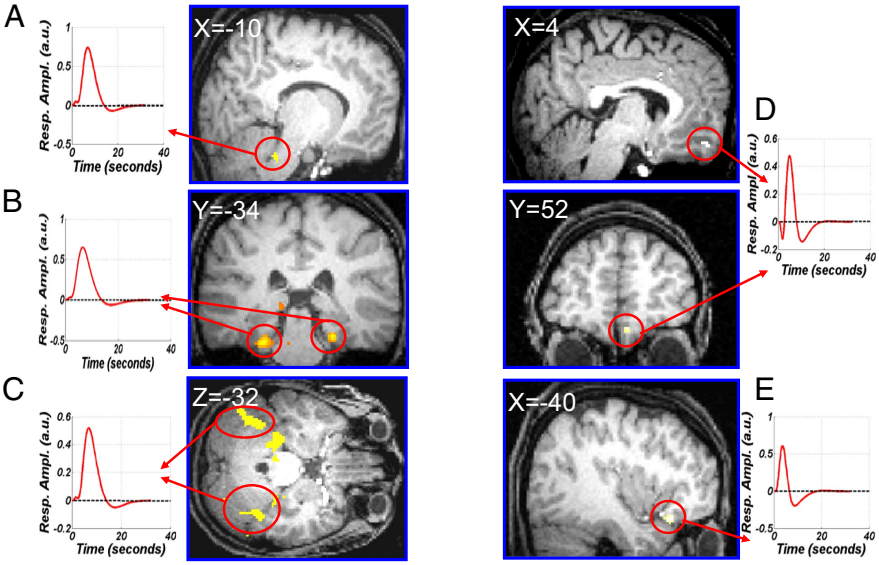

Fig. 3. fMRI results. Brain regions activated in relation to slow oscillation: specific effects of high-amplitude slow waves and delta waves. (*A–C*) Significant responses associated with slow waves. (*D* and *E*) Significant responses associated with delta waves. In both the slow wave and delta wave graphs, the side curves represent the time course (in seconds) of fitted response amplitudes (in arbitrary units) during slow waves or delta waves in the corresponding circled brain area. All responses consist of regional increases in brain activity. Functional results are displayed on an individual structural image (display at $P < .001$, uncorrected), at different levels of the *x*, *y*, and *z* axes, as indicated for each section. (*A*) Pontine tegmentum. (*B*) Parahippocampal gyrus. (*C*) Cerebellum. (*D*) Medial prefrontal cortex. (*E*) Inferior frontal gyrus.

tified in discrete cortical areas (i.e., inferior frontal gyrus, middle frontal gyrus, medial frontal gyrus, precuneus, posterior cingulate, and parahippocampal gyrus). This observation does not imply that the rest of the cortex does not participate in the slow oscillation. Our analysis characterized the activity consistently associated with detected slow waves and/or delta waves across subjects rather than responses elicited by each individual wave, the site of origin and pattern of propagation of which can vary (7). In the frontal lobe, activity associated with SWS waves included the medial, orbital, inferior, and middle frontal gyri but not with the superior frontal gyri. The recruitment of parietal and temporal association areas was much less extensive and was restricted to the precuneus. These findings are globally consistent with the pattern of origin of slow oscillation characterized by scalp EEG recordings. Slow oscillation seldom originates from posterior areas but is frequently initiated in frontal regions corresponding to the transition between the dorsolateral prefrontal and orbitofrontal cortex (7).

We identified slow oscillation-related activity in cortical areas that had not been identified by EEG recordings, especially limbic areas (parahippocampal gyrus). The bilateral activation in the parahippocampal gyrus is consistent with cellular firing patterns reported in animals during deep NREM sleep. At the cellular level, hippocampal activity is partially influenced by and synchronized to the cortical slow oscillation (17). Simultaneous activation of neural assemblies in the cortex and hippocampus during slow oscillation are thought to underpin memory processing (18). In humans, the hippocampus is activated during NREM sleep after training to memory tasks (19, 20), and slow oscillation has been proposed to play a key role in NREM sleep-associated consolidation of memory (21). In the present experiment, subjects were not submitted to any systematic memory task before sleep. Our results demonstrate that even under these conditions, slow oscillation is associated with consistent responses in the parahippocampal gyrus, a major relay area between the hippocampus and neocortex (22).

We detected increased activity in relation to slow oscillation in both cerebellar hemispheres and the vermis. Functional changes in the cerebellum during human NREM sleep have been reported, but as a decrease in activity (12). The participation of the cerebellum in the slow oscillation has not yet been characterized at the cellular level. A systematic investigation should explore whether the cerebellum actively contributes to generation of the slow oscillation or whether the slow oscillation passively follows the activity generated in thalamocortical loops.

Finally, we unexpectedly found significant responses associated with slow oscillation in the midbrain and pontine tegmentum, a region that includes critical structures involved in the regulation of sleep and wakefulness (especially cholinergic and aminergic nuclei) (1). In particular, the activated pontine area encompasses the locus coeruleus (LC), a noradrenergic nucleus located in the lateral floor of the fourth ventricle. This finding contrasts with the classical view of a necessary decrease in activity in the brainstem-activating systems for NREM sleep oscillations to emerge (1) and with the blockage of slow oscillation by stimulating cholinergic or noradrenergic brainstem structures (23). Consistent with preliminary results showing that the firing of LC neurons is organized by the cortical slow oscillation in rats (24), our data suggest that several structures in the brainstem, including the LC, may be active in phase with slow oscillation and may contribute to modulating cortical function during SWS.

The slow oscillation is known to synchronize thalamic firing sequences (25). Moreover, thalamic cells present intrinsic properties that give them the capability to generate a slow rhythm (26, 27). The absence of any thalamic response associated with slow waves or delta waves may appear to be at odds with these neurophysiological data. This negative finding is related to technical issues. The variance in thalamic voxels has been explained by regressors that account for activity related to sleep spindles and attributed to the nonlinearity of BOLD responses for high-frequency events (Volterra series; see *Materials and Methods*). The lack of thalamic response illustrates the conservativeness of the present analysis.

Slow and Delta Waves: Common or Distinct Processes? Whether the difference between slow waves (<1 Hz) and delta waves (1–4 Hz) is qualitative or quantitative remains unclear. In the former case, slow waves and delta waves represent two coalescent but distinct

Table 3. Brain regions specifically activated in relation to delta waves

Brain region	*x*	*y*	*z*	*P*	*Z* score
Right medial frontal gyrus (41)	4	52	−20	0.033	3.54
Left inferior frontal gyrus (13)	−40	22	−20	0.017	3.74

Here the *x*, *y*, and *z* values are coordinates in the MNI. The *Z* scores result from the statistical parametric analysis; *P* refers to the probability of the null hypothesis (i.e., absence of activity change associated with delta waves; $P < .05$), after correction for multiple comparisons on a volume of interest centered on published coordinates (reference specified for each brain area). Additional results that did not survive correction for multiple comparisons are given in Table S3.

rhythms. Whereas slow rhythm is strictly generated within cortical circuits, delta rhythm may be derived from intrinsic properties of thalamocortical cells as well as from intracortical network interactions (1). In keeping with this concept of slow waves and delta waves as distinct processes, EEG power densities within slow and delta frequency bands differ in their dynamics through the night: The latter decline from the first to the second NREM sleep episode, whereas the former do not (5).

The other hypothesis views slow waves and delta waves as realizations of a unique process, the slow oscillation, which varies in a continuous parameter space. The amplitude and slope of the waves reflect the level of synchronization achieved in cortical neural ensembles, which depends on the local homeostatically regulated average synaptic strength (10).

In this study, we arbitrarily distinguished two types of waves according to their respective amplitude. Slow waves and delta waves were defined not as EEG activities within specific frequency bands, but rather as individual events defined by amplitude per duration criteria. A peak-to-peak amplitude of >140 μV characterized high-amplitude slow waves (7), whereas the amplitude of delta waves was between 75 and 140 μV (Fig. 1*D*) (9). In keeping with the second ("quantitative") hypothesis, no significant difference in brain activation was found when comparing slow waves and delta waves at the macroscopic systems level; however, compared with baseline, slow waves and delta waves were seen to be related to distinct response patterns. Slow waves activated the rostral pons, cerebellum, and parahippocampal gyrus bilaterally (Fig. 3, *Left*), whereas delta waves were characterized by the activation of the inferior frontal gyrus and medial frontal cortex (Fig. 3, *Right*). One interpretation of these results is that the mesiotemporal areas, brainstem, and cerebellum are consistently recruited during a slow wave only under conditions of substantial cortical synchronization (leading to high wave amplitude), whereas the frontal areas participate in a slow wave even when cortical synchronization is less prominent (leading to lower wave amplitude). In line with this assertion, brain responses associated with slow waves or delta waves were found to be significantly modulated by the amplitude of the waves in the posterior hippocampus, pons, cerebellum (positive modulations), and inferior frontal gyrus (negative modulation) (data not shown).

Resting State Networks During SWS. Some previous independent studies consistently found a common pattern of brain activity during resting wakefulness relative to various active goal-directed behaviors (28). In this set of brain areas, commonly referred to as the "default mode" network (29), as well as in other large-scale cerebral networks, the fMRI BOLD signal spontaneously fluctuates at a frequency <0.1 Hz (30).

NREM sleep often is considered a resting state for the brain. In addition, spontaneous BOLD fluctuations seem to persist within the default mode network in humans during light NREM sleep (31). Finally, some of the cortical areas reported in the present study represent core components of the default mode network, namely the precuneus, posterior cingulate, and medial prefrontal cortices. These points suggest some functional commonalities between resting spontaneous BOLD fluctuations and the responses associated with SWS oscillations. This assumption remains controversial, however. On one hand, the partial spatial overlap between SWS-associated responses and spontaneous BOLD fluctuations does not imply that similar neural processes are in place. Here we have shown that regional brain activity is shaped by the slow rhythm during SWS. This fundamental electrical oscillation of NREM sleep is identified on EEG recordings by large-amplitude, low-frequency waves, the fundamental frequency of which is an order of magnitude larger than ultra-slow fMRI BOLD spontaneous fluctuations. The neural underpinnings of the slow rhythm have been characterized in increasing detail by using unit recordings in animals. In contrast, the neural correlates of spontaneous fluctuations of BOLD activity remain unknown. They have been correlated with the modulation of EEG power in various frequency bands during the waking resting state in humans (32) and in the delta frequency band in anesthetized rats (33). The spontaneous BOLD activity may just as likely be related to an elusive ultra-slow (<0.1 Hz) oscillation identified in humans on scalp EEG recordings (34).

On the other hand, up states of the slow oscillation recently have been characterized as microwake "fragments" that facilitate neuronal interaction and information processing in the sleeping brain (35). In this sense, one may wonder to what extent the brain responses associated with SWS oscillations reinstate the large-scale functional organization observed during the waking resting state at the cellular and macroscopic systems levels.

Conclusions

By using EEG/fMRI in non-sleep-deprived normal volunteers, we characterized the brain areas that consistently increased their activity in relation to SWS waves. Further studies using EEG or magnetoencephalography should specify how these various areas are recruited during individual slow waves and delta waves. Our results indicate that the involvement of mesiotemporal areas (i.e., hippocampus and parahippocampal gyrus) is related to wave amplitude, suggesting that the mesiotemporal areas are preferentially recruited in the context of substantial cortical synchronization. This finding has a potentially important bearing on our understanding of memory processing during NREM sleep and merits further investigation at the cellular and systemic levels.

The cortical areas that are consistently recruited by SWS waves partially overlap with the default mode network reported during resting wakefulness. This finding has potentially important implications for our understanding of information processing during NREM sleep. The extent to which transient surges in activity associated with SWS waves restore neural activity patterns and a neuromodulatory context suggestive of microwake fragments should be investigated in more depth.

Materials and Methods

Subjects. Twenty-five healthy, right-handed subjects (11 females; age range, 18–25 years; mean age, 21.96 years) gave written informed consent and received financial compensation for their participation in this study, which was approved by the Ethics Committee of the Faculty of Medicine, University of Liège. No participants had any history of medical, traumatic, psychiatric, or sleep disorders, as assessed by a semistructured interview. All participants were nonsmokers, moderate caffeine and alcohol consumers, and on no medications. Before the experimental night, the participants followed a 4 day constant sleep schedule, assessed by wrist actigraphy (Actiwatch; Cambridge Neuroscience) and sleep diaries. They were not sleep-deprived.

EEG Acquisition and Analysis. The EEG caps included 62 scalp electrodes online-referenced to FCz, as well as one electro-oculogram channel and one electrocardiogram (ECG) channel. By using abrasive electrode paste (ABRALYT 2000; FMS), electrode-skin impedance was kept <5 kohms, in addition to the 5-kohm resistor built into the electrodes. EEG was recorded in the scanner room simultaneously with fMRI acquisition during the first half of the night, by using two magnetic resonance (MR)-compatible 32 channel amplifiers (BrainAmp MR plus; Brain Products) and a MR-compatible EEG cap (BrainCap MR; Falk Minow Services) with 64 ring-type electrodes. Data were transferred outside the scanner room through fiberoptic cables to a personal computer, in which the EEG system running Vision Recorder Software, version 1.03 (Brain Products) was synchronized to the scanner clock. The EEG was digitized at a 5000 Hz sampling rate with 500 nV resolution. Data were analog-filtered by a band-limiting low-pass filter at 250 Hz (30 dB per octave) and a high-pass filter with a 10 s time constant corresponding to a high-pass frequency of 0.0159 Hz. For the offline analysis, EEG data were low-pass filtered (FIR filter; -36 dB at 70 Hz), down-sampled to 250 Hz, and re-referenced to the mastoids. Scanner gradient artifacts were removed by using adaptive average subtraction (36). Ballistocardiographic artifacts were removed by using an algorithm based on independent component analysis (37). Sleep staging followed standard criteria (9) and identified periods of stage 3 and stage 4 sleep, free of any artifacts, during which the EEG and fMRI data were analyzed. Only stable stage 3–4 epochs lasting >2 min were considered. Slow waves in these epochs were detected automatically, by using an algorithm adapted from Mas-

simini *et al.* (7). The detection algorithm was applied to potentials averaged over four large and nonoverlapping areas of the scalp (7): (1) F3, F1, Fz, F2, F4, FC1, and FC2; (2) FC5, FC3, C5, C3, C1, CP5, and CP3; (3) FC6, FC4, C6, C4, C2, CP6, and CP4; and (4) CP1, CPz, CP2, P3, P1, Pz, P2, and P4. The criteria for detecting the slow waves were applied independently to each local average (bandpass, 0.1–4 Hz) and were as follows (Fig. 1*D*): (1) a negative zero crossing and a subsequent positive zero crossing, separated by 0.3–1.5 s; (2) a positive zero crossing and a subsequent negative zero crossing, separated by <1 s; (3) a negative peak between the two zero crossings with voltage <-80 μV; and (4) a negative-to-positive peak-to-peak amplitude >140 μV. Delta waves were detected by using the same procedure but with different amplitude criteria (negative peak amplitude between -40 and -80 μV; peak-to-peak amplitude between 75 and 140 μV; Fig. 1*D*). Detected waves subsequently were checked visually for correct classification. The onset of the wave was set at the peak surface negativity, which is easily recognizable (Fig. 1*A*) and reflects the transition to the depolarizing phase of the intracellularly defined slow oscillation (4, 7). To take into account all identifiable neural events during SWS epochs, we also detected sleep spindles as described in ref. 38.

fMRI Data Acquisition and Analysis. To avoid movement-related EEG artifacts, the subject's head was immobilized in the head coil by a vacuum pad. The subject was asked to relax and try to sleep in the scanner whereas fMRI and EEG data were acquired continuously. The fMRI time series were acquired by using a 3-Tesla MR scanner (Allegra; Siemens). Multislice T2*-weighted fMRI images were obtained with a gradient echo-planar sequence by using axial slice orientation (32 slices; voxel size, $3.4 \times 3.4 \times 3$ mm; matrix size, $64 \times 64 \times 32$; time of repetition [TR], 2,460 ms; time to echo [TE], 40 ms; flip angle, 90°; delay, 0). Subjects were scanned during the first half of the night, starting at around midnight. A subject stayed until he or she indicated by button press the desire to leave, or for a maximum of 4,000 scans ($\approx$ 164 min). Functional volumes were analyzed by using Statistical Parametric Mapping 5 (SPM5; available from http://www.fil.ion.ucl.ac.uk/spm/software/spm5) implemented in MATLAB version 7.1 (Mathworks).

The fMRI time series were corrected for head motion, spatially normalized (two-dimensional spline; voxel size, $2 \times 2 \times 2$ mm) to an echo planar imaging template conforming to the Montreal Neurological Institute (MNI) space, and spatially smoothed with a Gaussian kernel of 8 mm full width at half maximum (FWHM). The analysis of fMRI data, based on a mixed-effects model, was conducted in two serial steps, accounting for intraindividual (fixed effects) and interindividual (random effects) variance. For each subject, the vectors, including slow wave and delta wave onsets, were convolved with the three canonical basis functions (hemodynamic response function, its derivative and dispersion) and used as regressors in the individual design matrix. To model all identifiable neural events of SWS, one vector containing sleep spindle onsets also was included for each session and convolved with the three canonical basis functions. To take into account the nonlinearity of the hemodynamic response for events separated by $<$ 1.5 s (which was the case for $\approx$ 20% of the detected slow wave/delta wave events), we included vectors representing interactions between regressors by using the Volterra series (39). To take into account artifacts related to cardiac cycle, an estimation of R-R intervals derived from the ECG was included as a regressor of no interest. Movement parameters estimated during realignment (translations in the *x*, *y*, and *z* directions and rotations around the *x*, *y*, and *z* axes) and a constant vector also were included in the matrix as variables of no interest. High-pass filtering was implemented in the matrix design by using a cutoff period of 128 s to remove low-frequency drifts from the time series. Serial correlations in the fMRI signals were estimated by using an autoregressive (order 1) plus white noise model and a restricted maximum likelihood algorithm. The main effects of the slow waves and delta waves were then tested by a linear contrast, generating a statistical parametric map [(SPM(T)]. These individual contrast images were then smoothed (6 mm FWHM Gaussian kernel) and entered in a second-level analysis. The second-level analysis consisted of an ANOVA with the basis set (three levels) and wave type (two levels) as factors. The error covariance was not assumed to be independent between regressors, and a correction for nonsphericity was applied. The resulting set of voxel values constituted maps of *F* statistics [SPM(F)], thresholded at $P < 0.001$ (uncorrected). To correct for multiple comparisons, statistical inferences were reported in regions of interest identified in neuroimaging studies of NREM sleep (see the tables) by using spherical volumes (10 mm sphere, i.e., $\approx$4000 mm^3; small volume correction), and a threshold of $P < .05$. Complete results at $P < .001$, uncorrected, are given in supporting information (SI) Tables S1–S3. Additional details on materials and methods are given in *SI Materials and Methods*.

ACKNOWLEDGMENTS. This work was supported by the Belgian Fonds National de la Recherche Scientifique (T.D., M.D., M.B., A.D., G.R., V.S., G.V., E.B., C.P., and P.M.), Fondation Médicale Reine Elisabeth (FMRE), the Research Fund of the University of Liège, the Interuniversity Attraction Poles Program-Belgian State-Belgian Science Policy, Erwin Schrödinger Fellowship J2470-B02 from the Austrian Science Fund (to M.S.), an Emmy Noether fellowship from the Deutsche Forschungsgemeinschaft (to S.G.), and le Fonds de la recherche en santé du Québec (J.C.).

1. Steriade M, McCarley RW (2005) *Brain Control of Wakefulness and Sleep* (Springer, New York).
2. Steriade M, Nunez A, Amzica F (1993) A novel slow ($<$ 1 Hz) oscillation of neocortical neurons in vivo: Depolarizing and hyperpolarizing components. *J Neurosci* 13:3252–3265.
3. Steriade M, Timofeev I, Grenier F (2001) Natural waking and sleep states: A view from inside neocortical neurons. *J Neurophysiol* 85:1969–1985.
4. Steriade M, Nunez A, Amzica F (1993) Intracellular analysis of relations between the slow ($<$1 Hz) neocortical oscillation and other sleep rhythms of the electroencephalogram. *J Neurosci* 13:3266–3283.
5. Achermann P, Borbely AA (1997) Low-frequency ($<$1 Hz) oscillations in the human sleep electroencephalogram. *Neuroscience* 81:213–222.
6. Molle M, Marshall L, Gais S, Born J (2002) Grouping of spindle activity during slow oscillations in human nonrapid eye movement sleep. *J Neurosci* 22:10941–10947.
7. Massimini M, Huber R, Ferrarelli F, Hill S, Tononi G (2004) The sleep slow oscillation as a traveling wave. *J Neurosci* 24:6862–6870.
8. Borbely AA (2001) From slow waves to sleep homeostasis: New perspectives. *Arch Ital Biol* 139:53–61.
9. Rechtschaffen A, Kales A (1968) *A Manual of Standardized Terminology, Techniques and Scoring System for Sleep Stages of Human Subjects* (Brain Information Service/Brain Research Institute, University of California Los Angeles).
10. Esser SK, Hill S, Tononi G (2007) Sleep homeostasis and cortical synchronization, I: Modeling the effects of synaptic strength on sleep slow waves. *Sleep* 30:1617–1630.
11. Raichle ME (2006) Neuroscience: The brain's dark energy. *Science* 314:1249–1250.
12. Maquet P (2000) Functional neuroimaging of normal human sleep by positron emission tomography. *J Sleep Res* 9:207–231.
13. Kaufmann C, *et al.* (2006) Brain activation and hypothalamic functional connectivity during human non-rapid eye movement sleep: An EEG/fMRI study. *Brain* 129:655–667.
14. Hofle N, *et al.* (1997) Regional cerebral blood flow changes as a function of delta and spindle activity during slow wave sleep in humans. *J Neurosci* 17:4800–4808.
15. Czisch M, *et al.* (2004) Functional MRI during sleep: BOLD signal decreases and their electrophysiological correlates. *Eur J Neurosci* 20:566–574.
16. Timofeev I, Grenier F, Bazhenov M, Sejnowski TJ, Steriade M (2000) Origin of slow cortical oscillations in deafferented cortical slabs. *Cereb Cortex* 10:1185–1199.
17. Isomura Y, *et al.* (2006) Integration and segregation of activity in entorhinal-hippocampal subregions by neocortical slow oscillations. *Neuron* 52:871–882.
18. Ji D, Wilson MA (2007) Coordinated memory replay in the visual cortex and hippocampus during sleep. *Nat Neurosci* 10:100–107.
19. Peigneux P, *et al.* (2004) Are spatial memories strengthened in the human hippocampus during slow wave sleep? *Neuron* 44:535–545.
20. Rasch B, Buchel C, Gais S, Born J (2007) Odor cues during slow-wave sleep prompt declarative memory consolidation. *Science* 315:1426–1429.
21. Marshall L, Helgadottir H, Molle M, Born J (2006) Boosting slow oscillations during sleep potentiates memory. *Nature* 444:610–613 .
22. Mohedano-Moriano A, *et al.* (2007) Topographical and laminar distribution of cortical input to the monkey entorhinal cortex. *J Anat* 211:250–260.
23. Steriade M, Amzica F, Nunez A (1993) Cholinergic and noradrenergic modulation of the slow (approximately 0.3 Hz) oscillation in neocortical cells. *J Neurophysiol* 70:1385–1400.
24. Yeshenko O, Moelle M, Marshall L, Born J, Sara SJ (2006) Locus coeruleus firing during SWS is time locked to slow oscillations: Possible contribution of the noradrenergic system to off-line information processing in rats. *J Sleep Res* 15(Suppl 1):11.
25. Contreras D, Destexhe A, Sejnowski TJ, Steriade M (1996) Control of spatiotemporal coherence of a thalamic oscillation by corticothalamic feedback. *Science* 274:771–774.
26. Blethyn KL, Hughes SW, Toth TI, Cope DW, Crunelli V (2006) Neuronal basis of the slow ($<$1 Hz) oscillation in neurons of the nucleus reticularis thalami in vitro. *J Neurosci* 26:2474–2486.
27. Hughes SW, Cope DW, Blethyn KL, Crunelli V (2002) Cellular mechanisms of the slow ($<$1 Hz) oscillation in thalamocortical neurons in vitro. *Neuron* 33:947–958.
28. Gusnard DA, Raichle ME (2001) Searching for a baseline: Functional imaging and the resting human brain. *Nat Rev Neurosci* 2:685–694.
29. Fox MD, Raichle ME (2007) Spontaneous fluctuations in brain activity observed with functional magnetic resonance imaging. *Nat Rev Neurosci* 8:700–711.
30. Damoiseaux JS, *et al.* (2006) Consistent resting-state networks across healthy subjects. *Proc Natl Acad Sci USA* 103:13848–13853.
31. Horovitz SG, *et al.* (2007) Low-frequency BOLD fluctuations during resting wakefulness and light sleep: a simultaneous EEG-fMRI study. *Hum Brain Mapp* 29(6):671–682.
32. Mantini D, Perrucci MG, Del Gratta C, Romani GL, Corbetta M (2007) Electrophysiological signatures of resting state networks in the human brain. *Proc Natl Acad Sci USA* 104:13170–13175.
33. Lu H, *et al.* (2007) Synchronized delta oscillations correlate with the resting-state functional MRI signal. *Proc Natl Acad Sci USA* 104:18265–18269.
34. Vanhatalo S, *et al.* (2004) Infraslow oscillations modulate excitability and interictal epileptic activity in the human cortex during sleep. *Proc Natl Acad Sci USA* 101:5053–5057.
35. Destexhe A, Hughes SW, Rudolph M, Crunelli V (2007) Are corticothalamic ''up'' states fragments of wakefulness? *Trends Neurosci* 30(7):334–342. Epub 2007 May 3.
36. Allen PJ, Josephs O, Turner R (2000) A method for removing imaging artifact from continuous EEG recorded during functional MRI. *NeuroImage* 12:230–239.
37. Srivastava G, Crottaz-Herbette S, Lau KM, Glover GH, Menon V (2005) ICA-based procedures for removing ballistocardiogram artifacts from EEG data acquired in the MRI scanner. *NeuroImage* 24:50–60.
38. Schabus M, *et al.* (2007) Hemodynamic cerebral correlates of sleep spindles during human non-rapid eye movement sleep. *Proc Natl Acad Sci USA* 104:13164–13169.
39. Friston KJ, Josephs O, Rees G, Turner R (1998) Nonlinear event-related responses in fMRI. *Magn Reson Med* 39:41–52.
40. Braun AR, *et al.* (1997) Regional cerebral blood flow throughout the sleep–wake cycle: An H2 (15)O PET study. *Brain* 120(Pt 7):1173–1197.
41. Maquet P, *et al.* (1997) Functional neuroanatomy of human slow wave sleep. *J Neurosci* 17:2807–2812.
42. Kajimura N, *et al.* (1999) Activity of midbrain reticular formation and neocortex during the progression of human non–rapid eye movement sleep. *J Neurosci* 19:10065–10073.
43. Dang-Vu TT, *et al.* (2005) Cerebral correlates of delta waves during non-REM sleep revisited. *NeuroImage* 28:14–21.